Exciton photon strong-coupling regime for a single quantum dot in a microcavity.

E. Peter, P. Senellart, D. Martrou, A. Lemaître, J. Hours, J.M. Gérard† and J. Bloch
CNRS-Laboratoire de Photonique et Nanostructures, Route de Nozay, 91460 Marcoussis, France
† *CEA/DRFMC/SP2M, Nanophysics and Semiconductor Laboratory,*
17 rue des Martyrs, 38054 Grenoble Cedex, France *
(Dated: December 3, 2004)

We report on the observation of the strong coupling regime between a single GaAs quantum dot and a microdisk optical mode. Photoluminescence is performed at various temperatures to tune the quantum dot exciton with respect to the optical mode. At resonance, we observe an anticrossing, signature of the strong coupling regime with a well resolved doublet. The Vacuum Rabi splitting amounts to $400\,\mu eV$ and is twice as large as the individual linewidths.

PACS numbers: 78.55.Cr, 78.67.Hc, 78.90 +t

ccsd-00003254, version 3 - 3 Dec 2004

Cavity Quantum Electrodynamics (CQED) has motivated a lot of fascinating experiments in Atomic Physics these last twenty years [1]. The spontaneous emission of light from atoms inserted in a microcavity can be controlled [2] and even become reversible in the so-called strong coupling regime (SCR) using high finesse cavities [3]. More recently, analogous CQED approach has been applied to the discrete states of semiconductor quantum dots (QD). The control of spontaneous emission with QDs inserted in microcavities has been observed [4, 5, 6, 7, 8, 9] and applied to the realization of efficient single photon sources [9, 10]. As in atomic physics [11], the SCR with an atomic-like QD state is of fundamental interest for new CQED experiments [12] but also for new solid state devices such as single QD lasers [13] or quantum logical gate. Indeed the discrete QD states could constitute the elementary building block of the solid-state quantum computer (referred to as qubits) [14, 15, 16] and the electromagnetic field of the cavity mode would mediate the interaction between qubits [17, 18].

When inserting a single QD inside an optical microcavity, two regimes can be reached, depending on the coupling strength between the QD exciton and the optical cavity mode [19]. In the weak coupling regime, the spontaneous emission rate of the QD exciton is modified as compared to outside the cavity. This phenomenon referred to as Purcell effect [20] has been observed for a QD inside a cavity [21, 22, 23]. In the SCR, the exciton-photon coupling is stronger so that the spontaneous emission becomes reversible. Photons emitted by the QD inside the cavity mode are re-absorbed, re-emitted... giving rise to the so-called one-photon Rabi oscillations. This coherent evolution takes place as long as the Rabi oscillation is faster than the decoherence due to both the exciton and the cavity mode. Until now, the SCR has not been observed for single QD in optical microcavity, either because the cavity losses are too large or the oscillator strength of the investigated QD (most of the times, InAs self-assembled QDs) is too small [8].

In the present letter we report on the first experimental observation of the strong coupling regime between a single QD and an optical microcavity mode. Using temperature tuning, we observe the spectral signature of mixed exciton photon states by photoluminescence. The quantum dots we use are quantum dots formed at the interface fluctuations of a thin GaAs quantum well. As theoretically predicted [24] and checked experimentally [25, 26], these monolayer fluctuation QDs have an oscillator strength much larger than InAs self-assembled QDs. For this reason, Andreani and co-workers have predicted that the SCR could be achieved when these QDs are inserted in a state-of-art micropillar. Here, we use another type of cavities, which present optical modes with even higher quality factors: microdisks supported by a small pedestal surrounded by air [27]. Within such microdisks, whispering gallery modes can establish: they are vertically confined by the large index contrast between semiconductor and air; they are guided in the circumference of the disk by total internal reflection [28].

Our sample was grown by molecular beam epitaxy on a GaAs substrate. Growth conditions were optimized to obtain large QDs, which are expected to present large oscillator strength [24]. After the buffer layer, a 10 minute annealing at 640 °C was performed under arsenic flow. Then a 1.5 μm layer of $Al_{0.8}Ga_{0.2}As$ was grown at low temperature (555°C). The growth temperature was raised to 600°C and a 71 nm short-period superlattice of 50 % mean Al composition was grown. Then, the active material was deposited: a 50 $nm Al_{0.33}Ga_{0.67}As$ barrier followed by a 13 monolayer (around 3.7 nm) GaAs QW was deposited, at a growth rate of 1.5 (resp. 1.0) Å.s^{-1} for the barrier (resp. QW). The growth temperature was then lowered to 590°C before depositing the top barrier (similar to the first one) to decrease element III interdiffusion. Finally the same 71 nm superlattice was grown on top of the structure to make it symmetric. A 120 s growth interruption was performed at each QW interface to smoothen the growth surface. We used a Scanning Tunneling Microscope (STM) coupled to the growth chamber to study the surface morphology at each interface. Figure 1c and 1d present STM picture of both interfaces just after the growth interruption. At the first

interface (fig. 1c), the surface is slightly rough with a few holes. On the opposite, after growth of 13 GaAs monolayers, the surface has become atomically smooth with no islands. In this sample, a monolayer fluctuation in the quantum well thickness resulting in a hole in the first interface $Al_{0.33}Ga_{0.67}As/GaAs$, or in an island in the second interface, creates an attractive potential (quantum dot) that can localize the centre of mass of the quasi 2D-exciton confined in the quantum well. Analysis of these STM images shows that the lateral size of the quantum dot is between 100 and 1 000 nm and that its areal QD density is around 10 μm^{-2}.

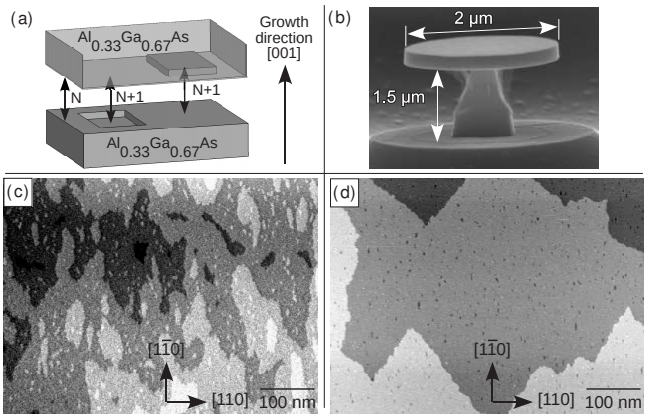


FIG. 1: (a) Schematic of a monolayer fluctuation QD. (b)Scanning electron microscopy sideview of a 2 μm diameter microdisk. (c) $800nm * 600nm$ Scanning tunnelling microscopy (STM) image of the surface after the deposition of the first 50 $nm Al_{0.33}Ga_{0.67}As$ barrier and after the growth interruption; the color changes correspond to one (AlGa)As monolayer changes in height (d), STM image of the surface after growth of the 13 monolayer GaAs QW and after the growth interruption.

To realize the optical microcavity, we performed an electron beam lithography followed by the lift-off of a 10 nm Ti mask in order to pattern an array of 3.8 μm diameter circular mesas. Then the sample was chemically etched by a non selective quasi isotropic solution (dichromate- based solution). After a vertical etching of 1.5 μm, the diameter of the disk is reduced by roughly 1.8 μm. Then, to define the microdisk pedestal, we perform a selective etching of the 1.5 μm Al rich layer using a diluted HF solution [27]. This last step also removes the Ti mask. Figure 1b shows a side-view of a typical 2 μm diameter microdisk constituting the optical cavity with the active layer inside.

Photoluminescence measurements are performed at a cryogenic temperature using a cold-finger helium cryostat. The excitation beam is delivered by a continuous wave Ti:Sapphire laser (of energy 1750 meV) focused with a microscope objective (numerical aperture 0.5) onto a 2 μm diameter excitation spot. The emission, collected at normal incidence by the same objective, is dispersed by a double grating spectrometer and detected with a N_2-cooled Si-CCD camera with a 80 μeV spectral resolution.

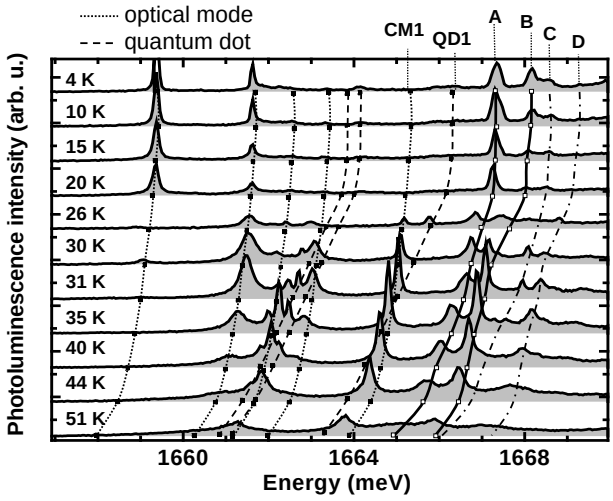


FIG. 2: Photoluminescence spectra (vertically shifted for clarity) on a single microdisk at various temperaturesfrom 4K to 51 K. The dotted (resp. dashed) lines are guides to the eye to follow the emission energy of the optical modes (resp. quantum dot excitons). Solid lines follow spectral shifts different both from a quantum dot and an optical mode spectral shift.

Figure 2 shows the spectra obtained on a single microdisk for various temperatures, between 4 K and 51 K. The observed luminescence peaks correspond either to the emission of quantum dots or to the emission of a small background within an optical cavity mode. Varying temperature allows identifying QDs versus optical modes. As previously reported [8], quantum dot emission energy exhibits a stronger spectral shift with temperature than an optical mode. The redshift of the QD when heating the sample is due to changes in the GaAs and $Al_{0.33}Ga_{0.67}As$ band gaps, whereas the redshift of the optical mode is due to the change of the microdisk AlGaAs index. The dashed lines (resp. dotted lines) on figure 2 follow the QD (resp. optical mode) emission energy. Because of this difference in temperature dependence, we can tune a QD exciton with respect to a cavity mode by changing the sample temperature. On figure 2, we observe seven whispering gallery modes within a 15 meV spectral window. This is consistent with the number of modes expected for a 2 μm diameter microdisk with 250 nm thickness at this wavelength.

Let us now consider the two lines labelled QD1 and CM1 on figure 2. At low temperature, QD1 is on the high-energy side of the cavity mode CM1. When increasing the temperature, the QD red-shifts more than the optical mode as is particularly visible at 26 K. Then a strong increase of the emission within the cavity mode CM1 is

observed around 31 K, temperature where QD1 and CM1 are in resonance. This QD is in the weak coupling regime with the cavity mode. At resonance, because of the Purcell effect, the QD emits photons preferentially within this mode. As a consequence, the emission intensity at the cavity mode energy is enhanced [21, 22, 23]. This intensity evolution with temperature would be completely different for a quantum dot not coupled to an optical mode: when increasing temperature, the emission also redshifts but simultaneously shows a progressive quenching of intensity because thermal heating results in exciton escape out of the quantum dot [29]. Notice also that around 1662 meV, we observe the resonance between two other QDs and two cavity modes.

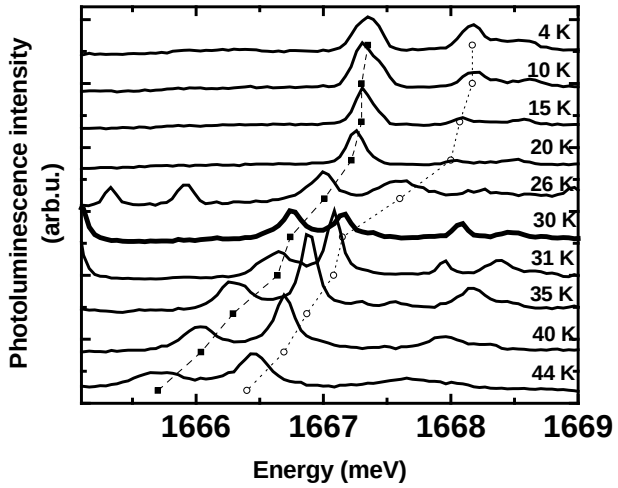


FIG. 3: Photoluminescence spectra (vertically shifted for clarity) for various temperatures between 4 K and 44 K. Dashed circles and squares: guide to the eye to follow the energy of the emission peaks for each temperature.

Consider now the emission peaks A and B on figure 2: this spectral shifts with temperature differ both from the typical exciton or optical mode behavior. A zoom of this region is presented on Figure 3. When increasing temperature from 4 K up to 30 K, the upper line shifts more than the lower line. This means that the upper line can be assigned to the quantum dot emission, and the lower line to a cavity mode. The emission linewidth of the lower line amounts to 0.2 meV, corresponding to a quality factor of 8000 for the considered whispering gallery mode. The emission linewidth of the upper line also amounts to 0.2 meV. This homogeneous broadening is not radiatively limited but due to dephasing mechanisms, such as phonon interaction [29, 30]. When increasing temperature, we do not observe a crossing as with QD1 and CM1, but an anticrossing, signature of the Strong Coupling Regime. Above 31 K, the lower line redshifts more than the upper line. The lower line is now assigned to the quantum dot and the upper line to the cavity mode. Because of the SCR, the eigenstates of the system are not the exciton and photon anymore, but two exciton-photon mixed states or dressed states, whose mixing depends on temperature. Let us underline that these measurements are performed at low excitation power, far below the QD saturation so that the mean photon number within the cavity mode remains below unity. We observe the coupling between an exciton and a single photon and the observed splitting is the Vacuum Rabi Splitting.

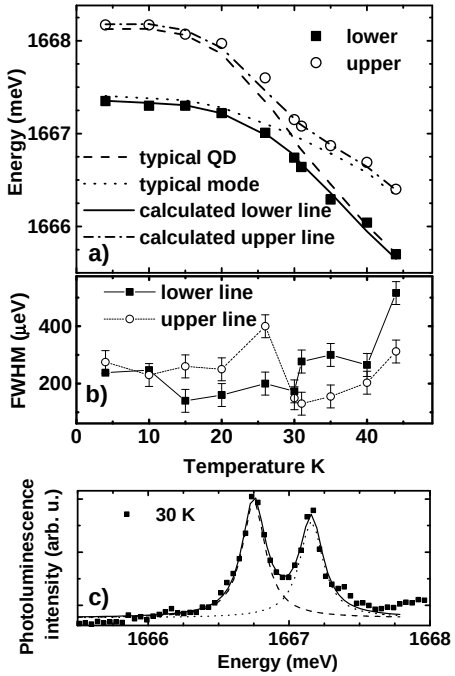


FIG. 4: (a) Symbols : emission energy of the upper and lower lines as a function of temperature. Dashed (resp. dotted) line: typical spectral shift of a quantum dot (resp. cavity mode). Continuous and dashed dot line : calculated energy of the two coupled states. (b) Emission linewidth of the lower (squares) and upper (circles) lines as a function of temperature. (c) Squares : Emission spectrum at resonance showing the Rabi doublet. Dashed and dotted lines: lorentzien fit of each peak. Continuous line: sum of the two lorentzien lines.

Figure 4a summarizes the emission energy of the upper and lower lines as a function of temperature. We also reported the typical spectral shift of a quantum dot (dashed line) and a cavity mode (dotted line). The minimum value of the measured splitting between the two peaks amounts to 400 μeV. Considering a coupling constant g = 200 μeV, we can calculate the energy of the two coupled states using [19]:

$$E_{\pm}(T) = \frac{E_C(T) + E_{QD}(T)}{2} \pm \frac{1}{2}\sqrt{(E_C(T) - E_{QD}(T))^2 + 4g^2} \quad (1)$$

where $E_C(T)$ and $E_{QD}(T)$ are the energy of the uncou-

pled cavity mode and QD exciton as shown from fig. 4a. We obtain a very good agreement with the experimental temperature dependance of the lower and upper lines.

Figure 4c shows the measured doublet at resonance. Notice that the two components have the same intensity. On the opposite, out of resonance the signal is different for the quantum dot and for the whispering gallery mode. This is due to their different emission pattern within the microscope objective. Since at resonance, both states are exactly half-exciton half-photon, they present the same radiation pattern. As a result, the equal intensities we observe within the doublet at resonance is another signature of the mixed nature of the eigenstates. At resonance, the two lines of the doublet present the same linewidth of 200 μeV. Theoretically, as both QD and cavity mode lines are homogeneously broadened, the linewidth of the mixed state is expected to be the sum of the exciton and photon linewidth weighted by the exciton and photon component of the mixed state. As temperature is increased, the photon like state (lower line below 30K, upper line above) linewidth remains unchanged and the QD-like state (upper line below 30K, lower line above) undergoes a thermal broadening [29]. At resonance, the linewidth of the two eigenstates is simply given by: $\frac{\gamma_{QD}+\gamma_{CM}}{2}$ where γ_{QD} and γ_{CM} are the QD and cavity mode linewith at the resonance temperature. As shown in fig. 4b, around 25K, the upper line (exciton like state) is thermally broadened and then gets narrower around 30K because of the strong exciton-photon mixing. This analysis in terms of mixed states explains the spectral narrowing of the upper line observed around the resonance temperature.

We now discuss the measured value of the Vacuum Rabi splitting. The coupling constant of the exciton-photon interaction is given by [24] :

$$g = \left(\frac{1}{4\pi\varepsilon_0\varepsilon_r} \frac{\pi e^2 f}{mV} \right)^{\frac{1}{2}} \qquad (2)$$

f is the exciton oscillator strength, V the effective modal volume, m the free electron mass, e the electron charge and $\varepsilon_0\varepsilon_r$ the dielectric constant. With a 2 μm diameter microdisk, $V \sim 6(\frac{\lambda}{n})^3$, where n is the effective refraction index of the cavity and λ the emission wavelength. With the experimental Rabi splitting, we deduce an exciton oscillator strength of $f = 100$, a value comparable to values experimentally measured [25, 26]. This value$f = 100$ is actually a minimum value since there may be a spatial mismatch between the QD and the optical mode antinode which would result in a smaller coupling constant. Then, to account for the measured splitting, larger oscillator strength would be required. As Andreani and coworkers have calculated [24] and as we have checked experimentally [26], the oscillator strength of monolayer fluctuation QDs strongly depends on their lateral size. From ref.[24], an oscillator strength of 100 corresponds to a lateral diameter of either 6 nm or 22 nm. According to the STM image of the QW interface, the QD under study most probably presents a diameter of at least 22 nm. Notice that peak C and D on figure 2 also present an anticrossing with a similar Rabi splitting, as temperature is changed. So in the same microdisk, some QDs are in the SCR with an optical mode whereas others are not: this can be due to variations of the oscillator strength from dot to dot and also to their position relatively to an antinode of the electromagnetic field.

To conclude, we have demonstrated the Strong Coupling Regime between a large oscillator strength GaAs QDs and a high finesse microdisk mode. This cavity geometry presents several promising advantages: in addition to an easy fabrication process, extremely high quality factors can be achieved associated to small effective volumes. Recently we reported on the fabrication of similar microdisks supported by an AlOx pedestal [31]. This pedestal makes them very robust, avoid thermal heating and allows the fabrication of all desired sizes in the same process. It is going to be straightforward to insert GaAs QD in these microresonators and achieve the SCR with even smaller effective volumes. Finally, if several QDs are strongly coupled to the same optical mode, the QDs can easily be selectively excited in this microdisk geometry, as required for the manipulation of two qubits interacting via the electromagnetic field [17]. The observation of the SCR between a single QD and a microcavity opens the way toward further fundamental investigations of cavity quantum electrodynamics in a solid state system.

This work was partly supported by the "Région Ile de France" and the "Conseil Général de l'Essonne".

* emmanuelle.peter@lpn.cnrs.fr

[1] For a review, see , S. Haroche, Phys. Today. **42**, 24 (1989).
[2] P. Goy *et al*, Phys. Rev. Lett. **50**, 1903 (1983).
[3] R.J. Thompson *et al*, Phys. Rev. Lett. **68**, 1132 (1992).
[4] J. M. Gérard *et al*, Phys. Rev. Lett. **81**, 1110 (1998).
[5] B. Gayral *et al*, Appl. Phys. Lett. **78**, 2828 (2001).
[6] L.A. Graham *et al*, Appl. Phys. Lett. **74**, 2408 (1999).
[7] G. Solomon *et al*, Phys. Rev. Lett **86**, 3903 (2001).
[8] A. Kiraz *et al*, Appl. Phys. Lett. **78**, 3932 (2001).
[9] E. Moreau *et al*, Appl. Phys. Lett. **79**, 2865 (2001).
[10] C. Santori *et al*, Nature **419**, 594 (2002).
[11] C.J. Hood *et al*, Phys. Rev. Lett. **80**, 4157 (1998).
[12] J. McKeever *et al*, Nature **425**, 268 (2003).
[13] J. M. Gérard in Single Quantum Dots , Topics of Applied Physics, Editor P. Michler, Heildeberg, Springer Verlag, (2003).
[14] For a review, see Single Quantum Dots , Topics of Applied Physics, Editor P. Michler, Heildeberg, Springer Verlag, (2003).
[15] S.N. Molotkov, JETP Lett. **64**, 237 (1996).
[16] F. Troiani *et al*, Phys. Rev. B **62**, R2263 (2000).

[17] A. Imamoglu *et al*, Phys. Rev. Lett. **83**, 4204 (1999).
[18] T. Pellizari *et al*, Phys. Rev. Lett. **75**, 3788 (1999).
[19] C. Fabre in Confined Photon Systems, Springer, Berlin (1999).
[20] E. M. Purcell, Phys. Rev. **69**, 37 (1946).
[21] J. M. Gérard *et al*, Phys. Rev. Lett. **81**, 1110 (1998).
[22] L. A. Graham *et al*, Appl. Phys. Lett. **72**, 1670 (1998).
[23] M. Bayer *et al*, Phys. Rev. Lett. **86**, 8168 (2001).
[24] L. C. Andreani *et al*, Phys. Rev. B **60**, 13276 (1999).
[25] T. H. Stievater *et al*, Phys. Rev. Lett. **80**, 1876 (2002).
[26] J. Hours *et al*, Phys. Rev. B (submitted) .
[27] B. Gayral *et al*, Appl. Phys. Lett. **75**, 1908 (1999).
[28] S. L. McCall *et al*, Appl. Phys. Lett. **60**, 289 (1992).
[29] E. Peter *et al*, Phys. Rev. B. **69**, R041307 (2004).
[30] P. Borri *et al*, Phys. Rev. Lett. **87**, 157401 (2004).
[31] E. Peter *et al*, Appl. Phys. Lett., to be published.